First-Order Fermi Acceleration at a Continuous Compression

D. Ruffolo and P. Chuychai

Department of Physics, Chulalongkorn University, Bangkok 10330, THAILAND

Abstract

The first-order Fermi acceleration mechanism is generally envisioned as taking place at a shock. However, there are situations, such as the trailing edges of coronal mass ejections (CMEs) as they pass the Earth, where there is a substantial fluid compression and change in direction of magnetic field lines that has not yet evolved into a shock discontinuity; treatment of this region will be an important component of realistic simulations of particle acceleration and Forbush decreases due to CMEs. Compressions also occur in structured shocks, e.g., in foreshock regions. We examine the effects of first-order Fermi acceleration at a continuous compression with a changing magnetic field direction by numerically solving a transport equation for the distribution of particles in momentum, pitch angle, position, and time. We find that first-order Fermi acceleration yields steeper steady-state power law spectra for greater values of the radius of curvature of magnetic field lines (i.e., a wider compression region). We also determine the distribution of particles in space and pitch angle near the compression. In contrast to the case of a shock discontinuity, for a continuous compression we find a sudden and dramatic decrease in the phase space density of energetic particles along the direction normal to the compression region, which can only be understood in the context of pitch angle transport.

1 Introduction:

Now that numerical solutions of the pitch angle transport of cosmic rays are feasible for realistic, quiescent configurations of the interplanetary magnetic field (Ruffolo 1995; Hatzky, Schmidt, & Kallenrode 1997; Kocharov et al. 1998; Lario, Sanahuja, & Heras 1998), a next step is to simulate the effects of transient phenomena, such as coronal mass ejections (CMEs) and associated interplanetary shocks, on the transport and acceleration of energetic charged particles, with an eye toward a better understanding of the acceleration of particles out of the solar wind, further acceleration of particles previously accelerated near the Sun, Forbush decreases, and cosmic ray modulation. Recently, simulations of the effects of an ideal, plane-parallel, oblique shock on mildly relativistic particles have been performed in the context of pitch-angle transport (Ruffolo 1999), and can readily be incorporated into models of cosmic ray transport in the interplanetary magnetic field. However, to be realistic, models of CME effects should include the refraction of magnetic field lines to be more tightly wound downstream of the shock, and these field lines must straighten out to a more normal configuration behind the CME. The region where this occurs is the CME reverse compression, which has not yet evolved into a shock discontinuity. Treatment of this region will be an important component of realistic simulations of the aforementioned phenomena. Compressions with refracted magnetic fields are also present in shocks with a finite width, e.g., in the foreshock region.

In this work, we modify existing transport equations to permit a general magnetic field configuration in space with no restriction on the particle velocity. We then address the effects of a continuous fluid compression with an oblique magnetic field in the steady state. We model the magnetic field lines as hyperbolae and study the effect of the ratio, $R/\lambda_{\parallel}$, where R is the maximum radius of curvature of the magnetic field, $\lambda_{\parallel}$ is the scattering mean free path parallel to the field, and the limit $R/\lambda_{\parallel} \rightarrow 0$ corresponds to the case of oblique shock acceleration. Here we examine the steady-state spectral index of the particle distribution, as well as the distribution in space and pitch angle; the same techniques could treat a magnetic field configuration and particle distribution that varies in time.

2 Transport Equation:

A transport equation for a general magnetic field configuration, to first order in (U/c) where U is the fluid speed, was provided by Skilling (1975). Transforming this equation, and keeping terms only to first order
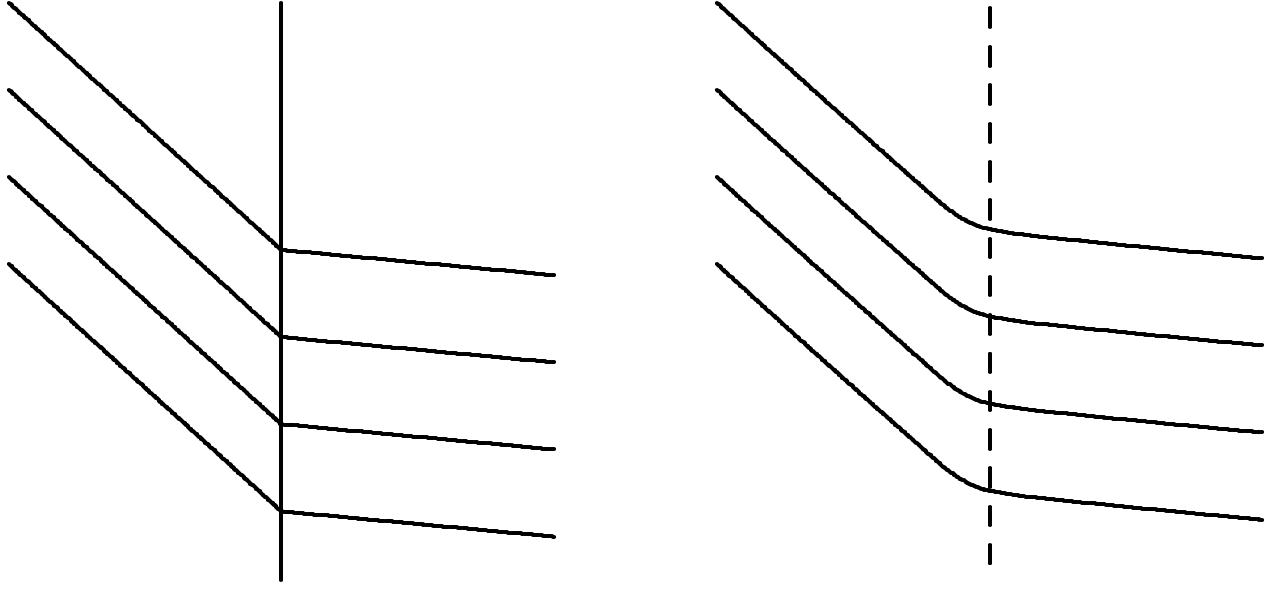
Figure 1: Left: Magnetic field lines for an idealized, plane-parallel shock. The vertical line indicates the shock plane. Right: Model configuration for a continuous compression. The field lines are hyperbolae, and the width of the transition region can be varied.

in (U/c) or (v/c), where v is the particle speed, and also keeping selected terms of higher order, one can obtain the transport equation of Kóta and Jokipii (1997). Inspired by that work, we have adapted the equation of Skilling (1975), retaining terms of general order in (v/c), to a form amenable to numerical solution as in Ruffolo (1995). Assuming a time-independent magnetic field, we have

$$
\begin{aligned}
\frac{\partial F}{\partial t} &= -\frac{\partial}{\partial z}\left[U_z + \mu v \ell_z - \frac{\mu^2 v^2 \vec{U}\cdot\hat{\ell}}{c^2}\ell_z\right]F \\
&\quad - \frac{\partial}{\partial p}p\left[\frac{1-3\mu^2}{2}\ell_i\ell_j\frac{\partial U_j}{\partial x_i} - \frac{1-\mu^2}{2}\vec{\nabla}\cdot\vec{U}\right]F \\
&\quad - \frac{\partial}{\partial \mu}\frac{1-\mu^2}{2}\left[v\vec{\nabla}\cdot\hat{\ell} + \mu\vec{\nabla}\cdot\vec{U} - 3\mu\ell_i\ell_j\frac{\partial U_j}{\partial x_i} - \frac{\mu v^2\vec{U}\cdot\hat{\ell}}{c^2}\vec{\nabla}\cdot\hat{\ell}\right]F \\
&\quad + \frac{\partial}{\partial \mu}\left[\frac{\varphi}{2}\frac{\partial}{\partial \mu}\left(1 - \frac{\mu v\vec{U}\cdot\hat{\ell}}{c^2}\right)F\right],
\end{aligned}
\tag{1}
$$

where $F(t,z,\mu,p) \equiv d^3N/(dpd\mu dz)$ is the particle distribution function, t is time in a fixed frame, z is a Cartesian coordinate in the fixed frame, e.g., along the shock normal, μ is the cosine of the pitch angle in the local fluid frame, p is the momentum in the local fluid frame, $\vec{U}(z)$ is the fluid speed, v is the particle speed in the local fluid frame, $\hat{\ell}(z)$ is a unit vector tangent to the magnetic field, and $\varphi(\mu)$ is the pitch angle scattering coefficient, which we assume to have the form $(v/\lambda_{\parallel})(1-\mu^2)$ corresponding to isotropic scattering.

Since we only treat motion along the magnetic field, one coordinate suffices to specify the location. For a time-dependent field configuration, to first order in (U/c) there would be corrections to the p- and μ-advection terms. With this equation, we can numerically study the pitch angle transport of particles subject to scattering from magnetic irregularities flowing with the fluid speed for a general static magnetic field; the equation of Skilling (1975) also includes terms which would enable one to extend the equation to permit time-dependent magnetic configurations.

3 Model Configuration:

Figure 1 shows the magnetic field lines for an idealized, plane-parallel shock and for our model of a continuous compression, with the upstream region on the right in both cases. The field lines are hyperbolae, and the fluid speed, taken to be in the z-direction (perpendicular to the ignorable coordinates), is such that the magnetic flux is "frozen" with the fluid. This permits analytic, albeit rather messy, expressions for all terms in the transport equation. The only parameters of the magnetic configuration are the asymptotic angles with respect to the z-axis (θ_1 upstream and θ_2 downstream) and the semi-conjugate axis of the hyperbola, b. We set $z = 0$ at the vertex, and the radius of curvature, which has a maximum there, is given by $R = b \cot \theta_h$, where $\theta_h = |\theta_1 - \theta_2|/2$. We take b and θ_1 as adjustable parameters, and for consistency with a shock configuration in the limit $b \to 0$, we use the magnetohydrodynamic jump conditions at the shock (de Hoffmann & Teller 1950) to determine θ_2. Results in the next section were for $\tan \theta_1 = 4$ ($\theta_1 = 76.0°$) and $\tan \theta_2 = 15.11$ ($\theta_2 = 86.2°$), derived for upstream Alfvén and sound speeds $u_{A1} = u_{s1} = 50$ km s^{-1}, and $U_1 = 144.3$ km s^{-1} (Ruffolo 1999).

4 Preliminary Results:

We found the spectral index which yielded a steady-state distribution function (neither increasing nor decreasing; Ruffolo 1999). Results for two continuous compression configurations and the limiting shock configuration (from previous work) are shown in Figure 2 (for $v = 0.5c$). We see that for this oblique magnetic field configuration, the spectral index steepens as the width of the compression region increases. A similar trend has been found for parallel magnetic field configurations (e.g., Krülls & Achterberg 1994).

Figure 3 shows the simulated pitch-angle averaged phase space density, $\langle f \rangle_\mu$, as a function of z in the steady state for two values of $b/\lambda_\parallel$. Note that since z is a Cartesian coordinate, f is proportional to F for a given p; here we normalize f to be one far downstream. Figure 3 indicates a sharp and dramatic decrease in the omnidirectional phase space density at the compression, which is sharper for the narrower compression width. This is in marked contrast to the case of an oblique shock (as $b/\lambda_\parallel \to 0$), for which $\langle f \rangle_\mu$ is nearly continuous, with only a slight jump ($\approx$3% for this configuration) to a higher value upstream (Os-
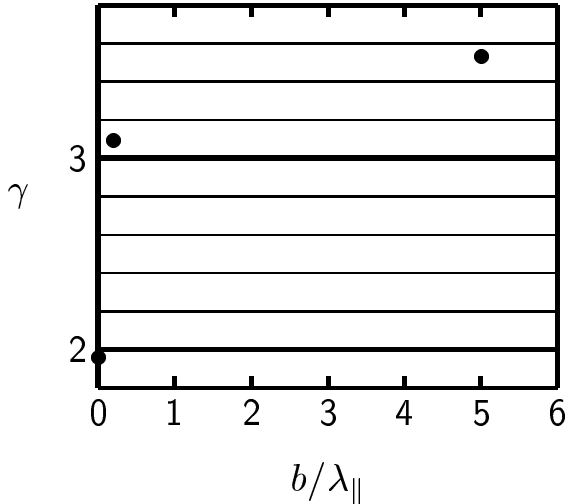

Figure 2: The spectral index vs. the ratio $b/\lambda_\parallel$, where b is the semi-conjugate axis of the hyperbolic magnetic field line, specifying the width of the compression, and $\lambda_\parallel$ is the scattering mean free path along the magnetic field.
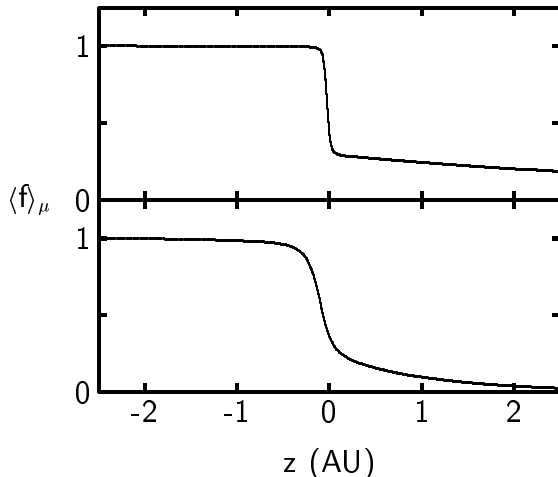

Figure 3: Pitch-angle averaged phase space density, $\langle f \rangle_\mu$ vs. z for $b = 0.2$ AU and $\lambda_\parallel = 1$ AU (upper panel) and for $b = 1$ AU and $\lambda_\parallel = 0.2$ AU (lower panel). The sharp drop in $\langle f \rangle_\mu$ at the compression is different from what is seen for a shock discontinuity; see text for details.

trowski 1991; Ruffolo 1999; Gieseler et al. 1999). The very different behavior we see here for continuous compressions cannot be understood in terms of the diffusion approximation. Instead, we believe that this is due to pitch angle scattering within the compression region, which results in increased transport from upstream to downstream. This in turn can explain the increased spectral index in the steady state, as greater momentum advection from lower p values is needed to maintain the greater downstream outflow. In further work, we will examine the acceleration time for such continuous compressions.

Acknowledgments:

References

de Hoffmann, F., & Teller, E. 1950, Phys. Rev., 80, 692

Gieseler, U. D. J., Kirk, J. G., Gallant, Y. A., & Achterberg, A. 1999, A&A, 345, 298

Hatzky, R., Kallenrode, M.-B., & Schmidt, J. M. 1997, Proc. 25th ICRC (Durban, 1997), 1, 245

Kocharov, L., Vainio, R., Kovaltsov, G. A., & Torsti, J. 1998, Sol. Phys., 182, 195

Kóta, J., & Jokipii, J. R. 1997, Proc. 25th ICRC (Durban, 1997), 1, 213

Krülls, W. M., & Achterberg, A. 1994, A&A, 286, 314

Lario, D., Sanahuja, B., & Heras, A. M. 1998, ApJ, 509, 415

Ostrowski, M. 1991, MNRAS, 249, 551

Ruffolo, D. 1995, ApJ, 442, 861

Ruffolo, D. 1999, ApJ, 515, 787

Skilling, J. 1975, MNRAS, 172, 557